EVS29 Symposium
Montréal, Québec, Canada, June 19 - 29, 2016

Magnetic Leakage Field Study of a 7 kW Wireless Electric Vehicle Charging System

D. Kuerschner[1] Member IEEE, G. Ombach[2] Senior Member IEEE,
L. Percebon[3] Member IEEE, S. Mathar[4] Member IEEE
QUALCOMM CDMA Technologies GmbH, Hollerithstraße 7a, 81829 Munich, Germany
[1] dkuersch@qti.qualcomm.com, [2] gombach@qti.qualcomm.com, [3] leandrop@qti.qualcomm.com,
[4] smathar@qti.qualcomm.com

Summary

This paper presents a study of the magnetic leakage field of a 7 kW wireless electric vehicle charging (WEVC) system. The leakage field was measured in different test configurations and environments. Typical system parameters, such as coil offset and air gap were evaluated in order to determine their influence on the leakage field distribution. All measured results were then validated by magnetic field simulations. Based on the results of this study, a magnetic leakage field assessment method based on simulation is proposed.

Keywords: EMC, inductive charger, wireless charging, electric vehicle (EV), simulation

1. Introduction

The majority of wireless electric vehicle charging (WEVC) systems are based on the principle of electromagnetic resonant induction, whereby the primary and secondary coils are tuned to a specific frequency. Most systems use a time-varying low frequency magnetic field in the frequency range of up to 100 kHz. The current in the primary coil of the resonant transformer creates an oscillating magnetic field around the primary coil. When a secondary coil is placed within this oscillating magnetic field, an electrical voltage is induced across its terminal. This voltage can be converted and then used to charge electric vehicle batteries.

WEVC includes both infrastructure and vehicle components. The infrastructure components consist of: a base charging unit (BCU), which includes a high frequency power supply (PSU) and a base pad (BP). The vehicle components consist of a vehicle charging unit (VCU) which includes the vehicle pad (VP) and an on-board controller. (Fig. 1).

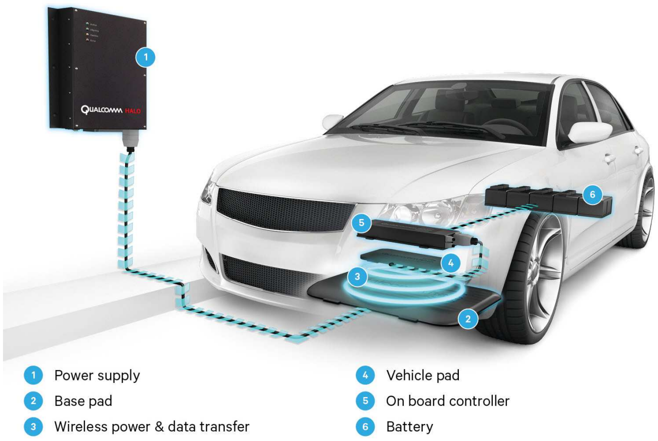

Fig. 1: WEVC system components.

The coils used for WEVC are magnetically loosely coupled due to the physical air gap between the primary coils in the BP and secondary coils in the VP [1-6]. The magnetic field between and around both coils can be differentiated into two parts: the magnetic main field and the magnetic leakage field. The magnetic main field is responsible for power transfer and it is characterized by the magnetic coupling factor k (typically k = 0.1 .. 0.3) [7-15]. The magnetic leakage field is inherent in inductive power transfer. It is generated by the WEVC system but does not contribute to the power transfer. Instead, the leakage field may cause unwanted electric and magnetic field exposure (EMF) and electromagnetic interference (EMI). In order to allow coexistence and electromagnetic compatibility (EMC) with electronic devices and implantable medical devices (IMD) as well as to ensure safe operation in terms of EMF exposure, the WEVC system must comply with existing standards and regulatory requirements. Therefore, the H leakage field around the WEVC system must meet defined emission limits at defined distances from the equipment under test (EUT) [20-23].

To better understand the WEVC system magnetic leakage field distribution, this paper investigates the leakage field of a 7 kW WEVC system by measurements and simulation. Measurements for different system configurations (e.g. charging system on a test rig vs. charging system on an actual car), at different system parameters (coil offset, lifted EUT etc.) and in different environmental conditions (e. g. EMC chamber, open air test site) were conducted. All measurements were then validated by magnetic field simulations using the FEM simulation software ANSYS Maxwell.

2. WEVC System Description

For the measurements and simulations conducted in this study, a 7 kW WEVC system, also referred to as EUT, comprised of a $(250x260x20)mm^3$ VP, a $(650x650x50)mm^3$ BP, a vehicle shield made of aluminum and primary and secondary power electronics, was used. A VP to BP distance of z = 95 mm was used (Fig. 2).

The considered frequency range was from the fundamental frequency of 85 kHz used by the EUT, up to the 10^{th} harmonic ($f \leq 850$ kHz). However, since in this study the fundamental frequency is always dominant compared to the frequency harmonics only the magnitude at fundamental frequency (85 kHz) is discussed in this paper. During the measurements the electrical power was kept at the nominal value (P_{out} = 6.6 kW) and all the pad currents and the currents phase-shift (φ_{I1I2}) as well as the battery voltage V_{bat} were tracked to allow reproducible measurements and simulations.

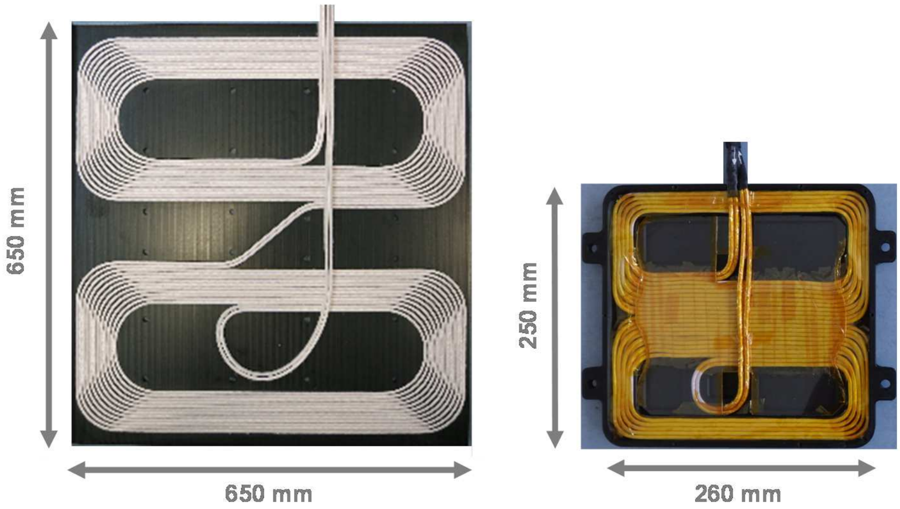

Fig. 2: BP (650x650x50)mm^3 (left picture) and VP (250x260x20)mm^3 (right picture) of the 7 kW WEVC system considered in this study.

3. Test Configuration

For EMC there are typically two different test configurations. First, a test rig configuration is used for an EMC characterization and comparison of different WEVC systems (component test). Second, a car configuration is used for an EMC characterization of one specific WEVC configuration at a specific system integration level (system test). Both configurations are subject of investigation in this paper. In particular, for all measurements and simulations conducted in this study, two configurations of the EUT were considered: mounted on a test rig and mounted on a BMW i3 vehicle. The test rig configuration was comprised of the VP, BP, the electronic parts and an (1.5x1.5)m^2 aluminium shield placed and centered above the VP. The power electronics (primary side inverter, secondary side rectifier, etc.) as well as the electronically controlled load were positioned separate from the test rig. The vehicle setup consisted of the WEVC system mounted on a BMW i3 car and feeding the car battery. In particular, the VP and a small vehicle shield were mounted on the car underbody. The VP was located close to the vehicle’s front axle and the on-board controller VCU was mounted on the car and all supply cables were twisted and shielded to allow focus on low frequency magnetic leakage fields only.

4. Test Environments

For each configuration, the EUT was tested in three test environments:

1) Semi-anechoic EMC chamber 1 (SAC1). Dimensions excluding absorbers: (20x12x7.7)m^3. Construction: metal ground floor, ferrite walls.
2) Semi-anechoic EMC chamber 2 (SAC2). Dimensions excluding absorbers: (25x16x8.7)m^3. Construction: metal ground floor and metal walls.
3) Open air test site (OATS). Contrary to EMC test standards [20, 21] no electrical conductive ground was used.

SAC1 and SAC2 differed in the size of the chamber and material used to construct the chamber. SAC1 was constructed with magnetically conductive (ferrite) walls and an electrically conductive floor. SAC2´s wall and floor were both electrically conductive. Fig. 4 shows some example pictures of the different test environments.

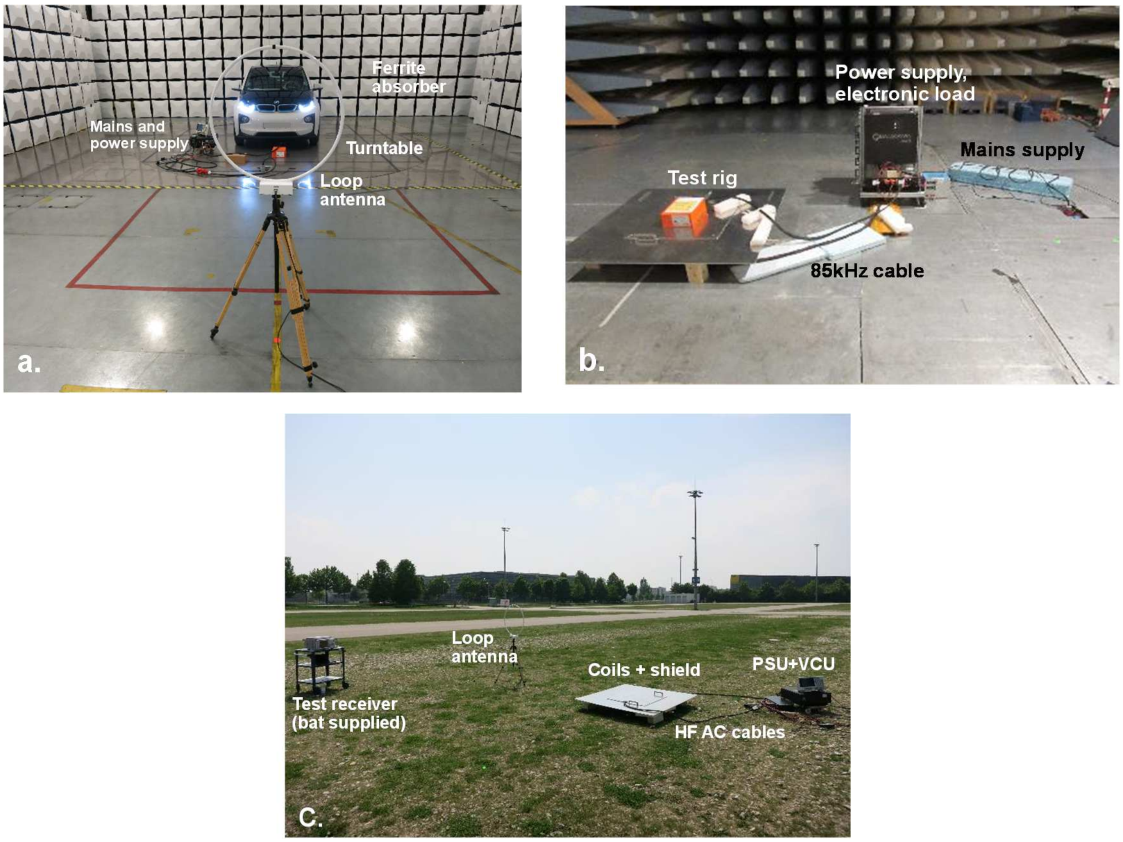

Fig. 4: Example measurement setups: a. 7 kW WEVC system mounted on BMW i3 car in SAC1; b. 7 kW WEVC system Test rig setup in SAC2; c. 7 kW WEVC system Test rig setup in OATS

5. Measurements

Fig. 5 illustrates all considered combinations of test environments and investigated EUT configurations and setup parameters. In addition to the test configurations and test environments described in Sections 3 and 4, the EUT configuration was tested at perfect coil alignment and at worst case offset conditions. Furthermore, the influence of the electrical conductive ground of the test environment was investigated by lifting the EUT by 10 cm as defined in EMC standards [20, 21]. This lifted EUT scenario was used to emulate steel reinforced concrete ground conditions. In all, over 260 system configurations were measured which resulted in the evaluation of more than 17,500 data points (incl. frequency components, H components, antenna correction factor etc.).

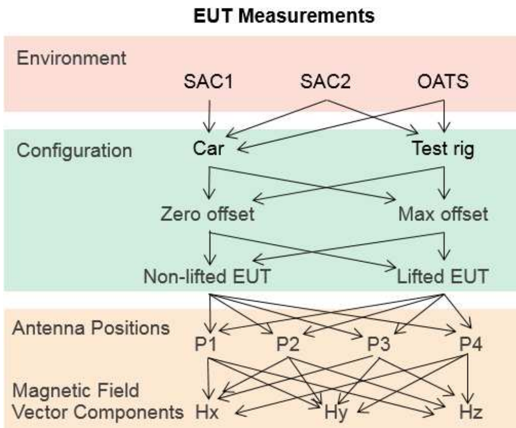

Fig. 5: The combinations of WEVC system configurations, parameters and test environments subject to measurement.

The leakage field was measured using a 60 cm loop antenna (Electro Metrics EM-6879) and an EMC test receiver (R&S ESRP3) using a Quasipeak detector as defined in [20, 21]. The loop antenna was placed at 1 m height above ground level and at a constant distance of 10 m from the EUT. In order to enable keeping this distance constant in the SAC environment, the BP was centred on the turntable. According to the EMC standards [20,21], the leakage field was measured for all magnetic field vector components (H_x, H_y, H_z) and for different antenna positions around the EUT; left - P1, right - P3, front - P2, back - P4, (Fig. 6). In the SAC environments, this was achieved by rotating the turntable in 90° increments and by keeping the antenna position constant. In the OATS environment, the antenna positions were set up manually and individually for all the four points around the EUT. For both, the coordinate system was always referenced to the test rig and/or to the vehicle orientation according to Fig. 6.

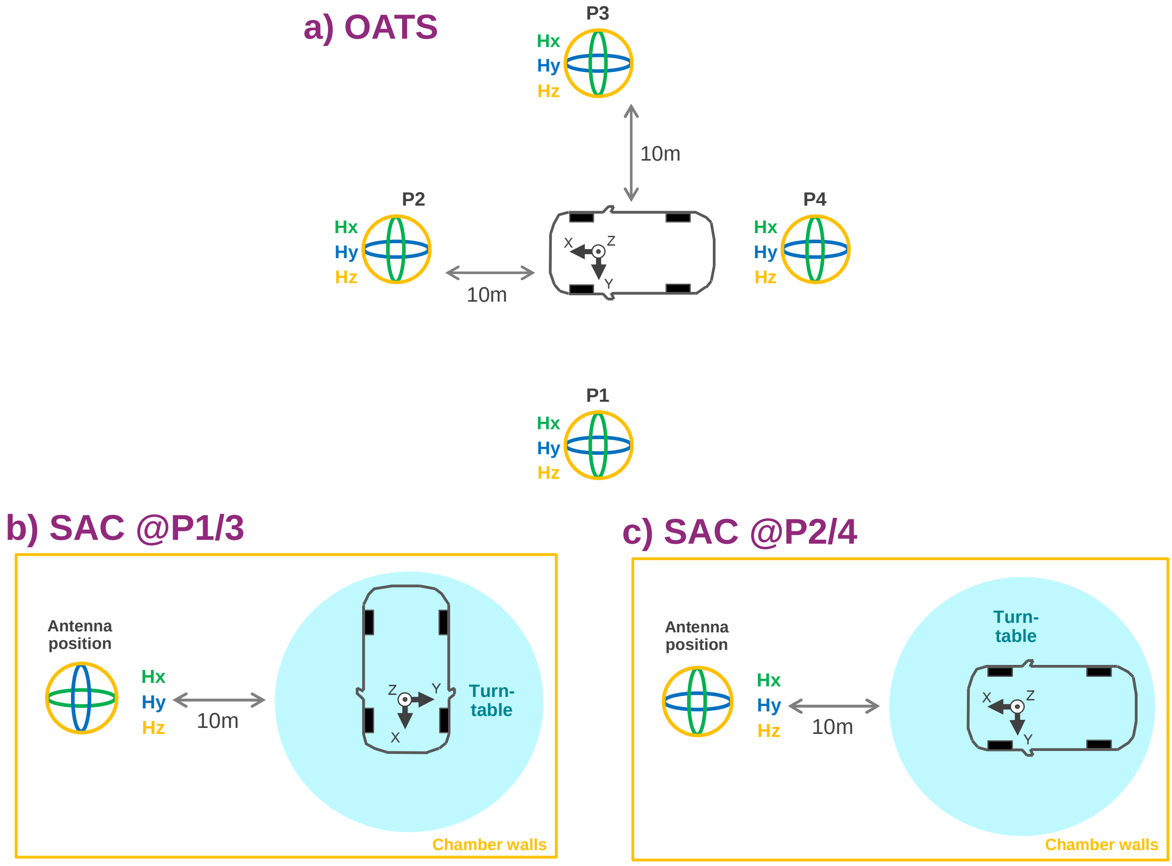

Fig. 6: Definition of measurement points and coordinate systems in different environments: a) OATS, b) SAC – for P1 and P3 antenna positions; c) SAC – for P2 and P4 positions.

Prior to the measurements, the worst case WEVC system configuration in terms of magnetic leakage field was determined by considering different test configurations (car vs. test rig) and system parameters (coil offset, battery voltage) and performing simulation according to the methodology presented in [24, 25]. For the WEVC system considered in this study, the worst case parameters were determined to be a coil offset of x = -75 mm, y = 100 mm and battery voltage of V_{bat} = 320 V.

Tab. 1 shows the maximum measured magnetic leakage field magnitudes (at the highest vector component H_x, H_y or H_z) for all considered environments and for all antenna positions (P1, P2, P3 or P4). It was found that the H_x vector component was dominant compared to the H_y and H_z vector components. The highest field magnitudes were located at P2 and/or at P4 antenna positions. It must be noted that this might be different for other WEVC coil topologies, measurement environments and loop antenna distances. The maximum measured magnetic field magnitude was 74.1 dBμA/m. The measurement results show that the test environment and the WEVC system configuration can significantly influence the emission magnitude level. For example, the measurement results in SAC2 showed in higher leakage field magnitudes of about 10 dB compared to the OATS environment. Aside from the influence of the test environment, the results also show a higher leakage field magnitude of additional 10 dB resulting from the different EUT configurations (test rig vs. car) and EUT parameters (offset, lifted EUT etc.). In particular and considering all measurement data, the leakage field magnitude increased by up to 4 dB for a test rig compared to car setup, increased by up to 5 dB for a coil offset configuration and increased by up to 1.5 dB for the configuration where the EUT was lifted by 10 cm above electrical conductive ground floor level (Tab. 2).

Tab. 1: Maximum leakage field over all antenna positions (P1, P2, P3 or P4) and over all magnetic leakage field vector components (H_x, H_y, H_z).

Location	EUT	Offset	EUT level	Hmax @10m
SAC1	Car	-75/100	not lifted	70.90
SAC2	Car	0/0	not lifted	71.20
		-75/100	not lifted	73.50
		0/0	lifted	61.20
		-75/100	lifted	74.10
	Test rig	0/0	not lifted	58.13
		-75/100	not lifted	71.11
		0/0	lifted	70.44
		-75/100	lifted	72.34
OATS	Car	0/0	not lifted	63.87
		-75/100	not lifted	65.73

Tab. 2: Influencing parameters on H leakage field magnitude.

Setup parameter	**Maximum difference**
Car vs. Test rig	< 4.0 dBμA/m
Offset: 0/0 vs. -75/100 mm	< 5.0 dBμA/m
EUT not lifted vs. EUT lifted	< 1.5 dBμA/m

6. Simulation

Magnetic field measurements require high effort in terms of time and cost. For this reason, the goal of this study was to validate measurements by simulations to allow emission characteristics for any WEVC system to be assessed in different environments and configurations by simulation. Therefore, each EUT measurement configuration and test environment considered in this study was modelled in ANSYS Maxwell, which is capable of simulating time-harmonic magnetic problems. It was found that it is important to use proper simulation domain and region size, specific boundary conditions, a reasonable meshing setup and correct assumptions for material properties and coil currents. For the simulations of the WEVC system considered in this study, the magnetic coils, ferrite layers and shield plates were modelled using the actual material properties of the Litz wire, soft ferrite and aluminium parts provided by data sheets [15-17]. The excitations of the BP and VP coil currents used were based on a coil current measurement. The BP and VP coils and the test rig and car were modelled according to the actual measurement configurations. The simulation models were also designed to emulate the real test environments. For the SAC1 test environment, the ground floor and walls were modelled as a box with walls made of a perfect magnetic conductor and a ground floor made of a perfect electrical conductor. The SAC2 test environment was modelled as a box with walls and ground floor made of a perfect electrical conductor. The OATS test environment was modelled as air by using a full sphere region. In order to enable the evaluation of the magnetic leakage field at the observation points at 10 m distance in the simulated OATS environment, a full sphere region domain with a diameter of d = 80 m was used. For both of the SAC environments, a box region was modelled using the actual measured chamber dimensions. For OATS, the EUT was always placed in the sphere region center and for both SAC the EUT was placed on the turntable center.

Fig. 7 shows the simulated magnetic leakage field distribution of the vector component H_z in SAC1 and in the height of 1.30 m above ground floor level as an example. Out of all the considered data points Tab. 3 summarizes the measured and simulated field magnitudes of the EUT configurations that resulted the highest differences between measurement and simulation. For these configurations, only the most relevant (highest) field vector component (H_x) as well as the worst case antenna position (P1, P2, P3 or P4) were considered. Tab. 3 shows that in the SAC2 and OATS environments, and when considering the relevant field magnitudes and vector components only, the maximum difference between measurement and simulation was below 3.6 dB. For the vector components with a relatively small field magnitude (H_y and H_z), the measurement and simulation differences can be significantly higher mainly due to the used FEM solver convergence properties. For SAC1, the maximum difference between measurement and simulation was initially determined to >7 dB which can be explained by the more complex physical effects in the ferrite absorber material of the chamber walls at low frequencies. As shown in Tab. 3, this correlation was improved to a maximum difference of 4.3 dB by increasing the model accuracy, in particular by using real meshed ferrite elements and modelling the actual ferrite material instead of perfect magnetic conductor properties. However, this option results in a significantly higher number of finite elements in the simulation model and therefore would result in a significantly higher overall simulation effort and time.

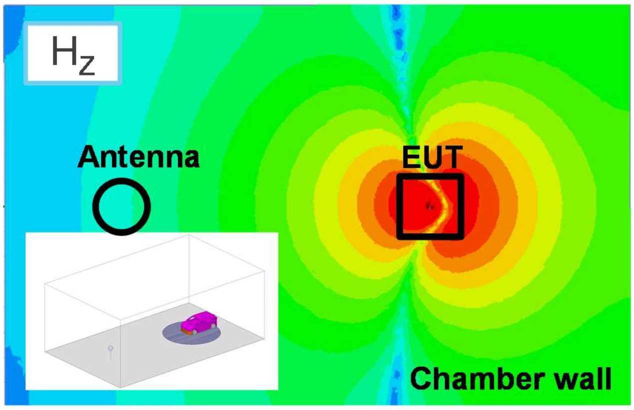

Fig. 7: Simulation of the magnetic vector field distribution (H_z) for SAC1. Top view of control plane @1.3 m above chamber ground level. Example setup: P2 antenna position for car configuration at maximum offset.

Tab. 3: Comparison of the simulated and measured magnetic leakage field magnitude for selected WEVC system configurations, parameter and test environments.

Test site	EUT setup	x/y offset / mm	EUT level / mm	Hmax @10m / dBµA/m Meas.	Sim.	Diff.
SAC1	Car	-75/100	0	70.90	66.56	**4.31**
SAC2	Car	0/0	0	60.40	57.78	**2.62**
		-75/100	0	62.60	60.13	**2.47**
		0/0	100	60.40	57.78	**2.62**
		-75/100	100	63.20	60.85	**2.35**
	Test rig	0/0	0	58.13	55.23	**2.90**
		-75/100	0	60.24	56.71	**3.53**
		0/0	100	70.44	66.86	**3.58**
		-75/100	100	61.42	57.83	**3.59**
OATS	Car	0/0	0	62.61	61.95	**0.66**
		-75/100	0	59.16	60.17	**1.02**

It is demonstrated that by using a proper modelling method (e. g. useful simulation domain and region size, boundary conditions, meshing setup, assumptions for material properties, etc.) a very good correlation between measurement and simulation can be achieved. Any difference between measurement and simulation can be explained by simulation model simplification (model approximation depth) and by measurement uncertainties. Therefore, it can be concluded and suggested that a WEVC system leakage field assessment can be conducted based on simulation only. Such a simulation assessment should include the determination of the worst case WEVC system configuration, the determination of the leakage field hot spot positions around the system to identify reasonable antenna positions and a final set of simulations to determine the actual leakage field magnitudes. In some cases, for validation purposes, measurements should also be conducted to confirm the simulation model and solver accuracy.

7. Conclusion

In this study, a 7 kW wireless electric vehicle charging (WEVC) system was measured and simulated in different configurations and test environments. A maximum magnetic leakage field of 74.1 dBµA/m was measured in an EMC chamber. It was found that test configurations, parameters and environments can significantly influence the leakage field magnitude. For the WEVC system considered in this study, the EMC chamber measurements showed higher leakage field magnitudes compared to an open area test site by about 10 dB. The test configuration (test rig vs. car setup), the coil offset or lifting the equipment under test above electrical conductive ground level were identified as resulting in an additional uncertainty of the leakage field magnitude by up to 10 dB.

The WEVC system configurations were modelled using the FEM simulation software ANSYS Maxwell. The correlation between measurement and simulation was very good and the maximum error was determined to be 3.6 dB.

Future work should focus on the influence of the test environment and the WEVC system configuration on the magnetic leakage field distribution. Addition investigations are planned.

References

[1] G. A. Covic and J. T. Boys: *Inductive Power Transfer.* Proc. IEEE, pp. 1-11, 2013

[2] T. Boys, G. A. Covic: *IPT Fact Sheet Series: No. 1 – Basic Concepts.* 2012 http://www.qualcomm.com

[3] M. Budhia, G.A. Covic, T. Boys: *Design and Optimization of Circular Magnetic Structures for Lumped Inductive Power Transfer Systems.* Power Electronics, IEEE Transactions on Volume: 26 , Issue: 11 Digital Object Identifier: 10.1109/TPEL.2011.2143730 Publication Year: 2011 , Page(s): 3096 - 3108

[4] M. Budhia, G.A. Covic, J.T. Boys, and C.Y. Huang: *Development and evaluation of single sided flux couplers for contactless electric vehicle charging*. Proc. IEEE Energy Conv. Cong., 2011, pp. 614-621

[5] O. H. Stielau and G. A. Covic: *Design of loosely coupled inductive power transfer systems.* Proc. IEEE POWERCON, 2000, pp. 85–90

[6] M. Yilmaz, P. Krein: *Review of charging power levels and infrastructure for plug-in electric and hybrid vehicles.* Electric Vehicle Conference (IEVC), 2012 IEEE International Digital Object Identifier: 10.1109/IEVC.2012.6183208 Publication Year: 2012 , Page(s): 1 – 8

[7] H. H. Wu, Hunter, A. Gilchrist, D. K. Sealy, P. Israelsen, J. Muhs: *A review on inductive charging for electric vehicles.* Electric Machines & Drives Conference (IEMDC), 2011 IEEE International Digital Object Identifier: IEMDC.2011.5994820 Publication Year: 2011 , Page(s): 143 – 147

[8] Hiroya Takanashi, Yukiya Sato, Yasuyoshi Kaneko, Shigeru Abe, and T. Yasuda: *A Large Air Gap 3 kW Wireless Power Transfer System for Electric Vehicles*. in IEEE Energy Conversion Congr. Exposition (ECCE), 2012

[9] I. Fujita, T. Yamanaka, Y. Kaneko, S. Abe, and T. Yasuda: *A 10 kW transformer with a novel cooling structure of a contactless powertransfer system for electric vehicles.* in IEEE Energy Conversion Congr. Exposition (ECCE), 2013, pp. 3643-3650

[10] M. Budhia, G. A. Covic , and J. T. Boys: *Design and Optimization of Circular Magnetic Structures for Lumped Inductive Power Transfer Systems.* IEEE Trans. Power Electron., vol. 26, pp. 3096-3108, 2011

[11] Y.Nagatsuka, N. Ehara, Y. Kaneko, S. Abe, and T. Yasuda: *Compact contactless power transfer system for electric vehicles*. IEEE Power Electron. Conf. (IPEC), 2010, pp. 807-813

[12] F. Y. Lin, A. Zaheer, M. Budhia, Grant A Covic: *Reducing Leakage Flux in IPT Systems by Modifying Pad Ferrite Structures*. IEEE Energy Conversion Congr. Exposition (ECCE), 2014, pp. 1770-1777

[13] Kürschner, D. ; Rathge, C. ; Jumar, U.: *Design methodology for high efficient inductive power transfer systems with high coil positioning flexibility.* IEEE Transactions on Industrial Electronics, Vol. 60, Issue: 1, 2013, p.372-381

[14] Kürschner, D. ; Rathge, C. ; Schulze, E.: *Optimization of contactless inductive transmission systems for high power applications.* Power Electronics Intelligent Motion Power Quality - PCIM, Nürnberg, 22.-24.05.2007, Proceedings on CD-ROM

[15] Kuerschner, D. ; Turki, F. ; Yotta, C. ; Thamm, S. ; Rathge, C.: *Comparison of Planar and Solenoid Coil Arrangements for Inductive EV-Charging Application.* PCIM, 14.–16.05.2013, Nuremberg, Germany, Proceedings p. 385-391, ISBN 978-3-8007-3505-1

[16] Ombach, G.; Kuerschner, D.; Mathar, S.; Chlebosz, W.: *Optimum magnetic solution for interoperable system for stationary wireless charging.* International Conference on Ecological Vehicles and Renewable Energies - EVER, 31.03.2015 - 02.04.2015, Monte-Carlo (Monaco)

[17] Ombach, G.; Kuerschner, D.; Mathar, S.: *Universal base coil solution for interoperable system for stationary wireless EV charging.* International Conference on Sustainable Mobility Applications - SMART, 23.-25.11.2015, Kuwait

[18] http://www.draysonracingtechnologies.com/ product.html?Wireless-Power-Transfer-Systems-6, 9/17/2014

[19] http://www.ipt-technology.com/index.php/en/about-us, 9/17/2014

[20] Industrial, scientific and medical equipment - *Radio-frequency disturbance characteristics - Limits and methods of measurement.* IEC/CISPR 11:2009

[21] Specification for radio disturbance and immunity measuring apparatus and methods - Part 2-3: *Methods of measurement of disturbances and immunity - Radiated disturbance measurements.* CISPR 16-2-3:2010

[22] ICNIRP - International Commission on Non-Ionisation Radiation Protection: *Guidelines for limiting exposure to time-varying electric and magnetic fields (1Hz-100kHz).* Health Physics 99(6): 818-836, 2010

[23] ANSI/AAMI PC69:2007 *Active implantable medical devices - Electromagnetic compatibility - EMC test protocols for implantable cardiac pacemakers and implantable cardioverter defibrillators.*

[24] J. Nadakuduti, M. Douglas, P. Crespo-Valero and N. Kuster: *Comparison of different safety standards in terms of human exposure to electric and magnetic fields at 100 kHz.* 33rd Annual Meeting of the Bioelectromagnetics Society (BEMS 2011), Halifax, Canada, June 12 - 17, 2011.

[25] J. Nadakuduti, M. Douglas, L. Lu, A. Christ, P. Guckian, N. Kuster: *Compliance Testing Methodology for Wireless Power Transfer Systems.* IEEE Transactions On Power Electronics, Vol. 30, No. 11, November 2015

Authors

Daniel Kuerschner received Diploma and Ph.D degrees in electrical engineering from the Otto-von-Guericke-University of Magdeburg in 2005 and 2009, respectively. He worked on wireless power transfer at the Institut f. Automation und Kommunikation (Magdeburg) from 2004-2011 and at Paul Vahle (Kamen) from 2011-2013. In 2013, he joined QUALCOMM CDMA Technologies GmbH and is responsible for simulation, design and EMC/EMF of wireless electric vehicle charging systems (WEVC). Daniel Kuerschner has more than 12 years' experience with inductive power transfer technology, particularly with magnetics, power electronics, electromagnetic compatibility and simulation methods. In these fields he has published more than 30 scientific papers. He is member of IEEE, SAE international and several German standardization committees, including VDE and DKE.

Grzegorz Ombach is the Vice President of Engineering at QUALCOMM CDMA Technologies GmbH and is responsible for global research and development of Qualcomm Incorporated's wireless electric vehicle charging (WEVC) technology. He joined Qualcomm in April 2012 from Brose Fahrzeugteile, where he managed the design of automotive electric drive systems as Director of Advanced Development Drives. Prior to Brose Fahrzeugteile, he was Principal Expert for Electromagnetic Simulation and Motor Design at Siemens VDO Automotive AG. His responsibilities included management of a panel of experts in charge of electric drive systems for automotive. Grzegorz Ombach holds a MSc. in electrical engineering from the Technical University of Lodz, Poland, and a Ph.D. in electrical engineering from the Silesian University of Technology, Poland. He has published over 70 papers and holds more than 25 patents (awarded and pending) on automotive electrical systems.

Leandro A. Percebon received the B.E. and M.Sc. degrees in electrical engineering from the Federal University of Santa Catarina, Florianópolis-Brazil in 2010 and 2012, respectively. After gaining his B.E., he worked at Engineering Simulation and Scientific Software (ESSS) where he was responsible for supporting electromagnetic simulation of different electromagnetic devices. In 2013, he joined QUALCOMM CDMA Technologies GmbH as a simulation expert. His responsibilities include simulation, design and analysis of wireless charging systems for electric vehicles (WEVC) and the areas of electromagnetic safety and interference.

Sebastian Mathar studied electrical engineering at RWTH Aachen University. He has a Ph.D in mechanical engineering, also from RWTH Aachen University. Sebastian Mathar is an expert for standardization of wireless electric vehicles charging (WEVC) systems. He has more than 10 years of experience in standardization work, and is a founding member of all major working groups in IEC, ISO and SAE which deal with WEVC standards. He joined QUALCOMM CDMA Technologies GmbH in 2013. Before that, he worked for an engineering services provider in the automotive industry in various leadership positions.